Inherent rheology of a granular fluid in uniform shear flow

Andrés Santos* and Vicente Garzó†
Departamento de Física, Universidad de Extremadura, E-06071 Badajoz, Spain

James W. Dufty‡
Department of Physics, University of Florida, Gainesville, Florida 32611, USA
(Received 15 September 2003; revised manuscript received 9 February 2004; published 10 June 2004)

In contrast to normal fluids, a granular fluid under shear supports a steady state with uniform temperature and density since the collisional cooling can compensate locally for viscous heating. It is shown that the hydrodynamic description of this steady state is inherently non-Newtonian. As a consequence, the Newtonian shear viscosity cannot be determined from experiments or simulation of uniform shear flow. For a given degree of inelasticity, the complete nonlinear dependence of the shear viscosity on the shear rate requires the analysis of the unsteady hydrodynamic behavior. The relationship to the Chapman-Enskog method to derive hydrodynamics is clarified using an approximate Grad's solution of the Boltzmann kinetic equation.

DOI: 10.1103/PhysRevE.69.061303 PACS number(s): 45.70.−n, 05.20.Dd, 05.60.−k, 51.10.+y

I. INTRODUCTION

Consider a fluid between parallel plates in the x,z plane separated by a distance L and with relative velocity U along the positive x direction. Given appropriate boundary conditions, the fluid undergoes simple shear with the local velocity field given by $u_x=ay$, $u_y=u_z=0$, where $a=U/L$ is the constant shear rate. The work done by the plates on the fluid near the boundaries tends to increase the temperature locally due to its viscosity. For normal fluids, this is compensated by a heat flux toward the center with a corresponding temperature gradient characterizing Couette flow in the steady state. A quite different steady state is possible for granular fluids where both the temperature and density fields are spatially uniform, called simple or uniform shear flow (USF) [1,2]. This is possible because the particle collisions in a granular fluid are inelastic and there is a continual loss of energy. This collisional cooling can compensate locally for the viscous heating so that no heat flux is generated. If the temperatures at the walls are not controlled the fluid autonomously seeks the temperature at which this exact balance between collisional cooling and viscous heating occurs. Otherwise, for fixed wall temperature one or the other will dominate leading again to Couette flow but with the curvature of the temperature field controlled by both mechanisms. This more general case has been discussed in detail elsewhere [3] including USF as a special case. Here, attention will be limited to the special features of USF.

The steady USF has been extensively studied. Molecular dynamics and Monte Carlo simulations [4–10] have been performed to measure the dependence of the stress tensor on the density and inelasticity. On the theoretical side, Lun *et al.* [11] have obtained the rheological properties of a dense gas for small inelasticity, while Jenkins and Richman [12] have used a maximum-entropy approximation to solve the Enskog equation. This method has been subsequently extended to highly inelastic spheres [13]. Sela *et al.* [14] have solved the Boltzmann equation to third order in the shear rate, finding normal stress differences. Some progress has been made by using model kinetic equations for dilute granular gases [15], as well as for dense granular gases [16]. Exact solutions derived in both cases compare quite well with Monte Carlo simulations, even for strong dissipation. Similar studies for multi-component systems are much scarcer, although some recent work has been carried out [10,17–19].

Normally, transport properties are defined for general states with the temperature, shear rate, and restitution coefficient as independent variables. For example, the shear viscosity as given by the Chapman-Enskog solution to the Boltzmann equation [20] has the form for shear flow $\eta=\eta(T,a,\alpha)$, and the Newtonian shear viscosity is obtained from it at zero shear rate, $\eta_0(T,\alpha)=\eta(T,a=0,\alpha)$. However, in the steady state of USF the condition for balancing collisional cooling and viscous heating implies that the steady state temperature is a function of the shear rate a and the coefficient of restitution α measuring the degree of inelasticity of the particles, $T_s=T_s(a,\alpha)$. In this case $\eta=\eta(T_s(a,\alpha),a,\alpha)=\eta_s(a,\alpha)=\eta_s'(T_s,\alpha)$. This complication raises two interesting questions:

(1) For sufficiently small a, is it possible to describe USF using Newtonian hydrodynamics?

(2) If $\eta_s(a,\alpha)$ is measured in USF, can the Newtonian viscosity $\eta_0(T,\alpha)$ be deduced from it?

The objective of this paper is to answer these two questions in the general context of hydrodynamics for granular fluids. It is shown that the answer is negative in both cases, implying that USF is inherently non-Newtonian and that the full nonlinear dependence of $\eta(T,a,\alpha)$ on the shear rate is required, even for small a, at any $\alpha\neq 1$. This result is important because it identifies a fundamental and unbridgeable gap

*Electronic address: andres@unex.es;
URL: http://www.unex.es/fisteor/andres/
†Electronic address: vicenteg@unex.es;
URL: http://www.unex.es/fisteor/vicente/
‡Electronic address: dufty@phys.ufl.edu;
URL: http://www.phys.ufl.edu/~dufty/

between Navier-Stokes hydrodynamics and the hydrodynamics for steady shear flow. There is no possibility of using USF to study the Newtonian viscosity (e.g., by molecular dynamics simulation); there is no possibility of using the Navier-Stokes equations to describe USF or states near it (e.g., the stability of USF). This is not an entirely negative result, however, because it shows that USF is a rich testing ground for the study of rheology. Any measurement will necessarily be illustrating some rheological effect.

These results may seem counterintuitive at first as with many conceptual differences between granular and real fluids. However, the steady state considered here for the granular fluid does not exist for a real fluid so intuition is not reliable in this case. The analysis presented here, and illustrated in detail for a dilute gas, is important because similar failures of the Navier-Stokes level hydrodynamics must be expected for other steady states specific to granular fluids. This peculiar limitation of Newtonian hydrodynamics may apply generically when the steady state exists only because of the internal cooling mechanism, rather than as a consequence of controllable external fields or boundary forces. The steady state implies the equivalence of spatial heat conduction, viscous heating, and collisional cooling, and a consequent relationship between the heat flux, momentum flux, and cooling rate (see below). For a given cooling rate (i.e., given restitution coefficient) the gradients of the hydrodynamic fields can no longer be controlled independently to assure the validity of the Newtonian limit. This phenomenon is elaborated further in the next section for USF based on the macroscopic balance equations for mass, energy, and momentum, and idealized boundary conditions for a general granular fluid. This analysis assumes only the existence of a hydrodynamic description, but is not limited to any small gradient, small inelasticity, or other approximation. A more detailed illustration from the Boltzmann kinetic theory is given in Sec. III. An important point of this kinetic theory analysis is the determination of the rheological equation of state $\eta(T,a,\alpha)$ for *both* steady and unsteady states of USF. In the unsteady state the temperature increases (decreases) depending on whether the viscous heating of the initial state is larger (smaller) than the collisional cooling. The three parameters a,α,T can be controlled independently, and there is a small shear rate domain for which the unsteady fluid is Newtonian. In the steady state, however, these parameters are constrained, $T=T_s(a,\alpha)$, such that $\eta(T_s(a,\alpha),a,\alpha)$ is never in its Newtonian limit for any $\alpha<1$. These results and their importance for the study of transport in granular fluids are summarized with comments in the last section.

II. HYDRODYNAMICS FOR USF

An idealized granular fluid consists of smooth hard spheres ($d=3$) or disks ($d=2$) of diameter σ and mass m. The collisions between particles are characterized through a constant coefficient of normal restitution α with values $0<\alpha\leqslant 1$. The elastic limit corresponds to $\alpha=1$. The exact macroscopic balance equations for mass, energy, and momentum are

$$D_t n + n\,\boldsymbol{\nabla}\cdot\mathbf{u}=0, \tag{1}$$

$$(D_t+\zeta)T+\frac{2}{dn}(P_{ij}\nabla_j u_i+\boldsymbol{\nabla}\cdot\mathbf{q})=0, \tag{2}$$

$$D_t u_i+(mn)^{-1}\nabla_j P_{ij}=0, \tag{3}$$

where n is the density, T is the granular temperature, $\mathbf{u}$ is the flow velocity, $D_t=\partial_t+\mathbf{u}\cdot\nabla$ is the material derivative, ζ is the cooling rate, P is the pressure tensor, and $\mathbf{q}$ is the heat flux. On physical grounds, ζ has essentially the form $\zeta\approx\nu(1-\alpha^2)$, where $\nu\propto\sqrt{T}$ is a mean collision frequency and $1-\alpha^2$ is the fraction of energy lost in each inelastic collision. In order to get a closed set of hydrodynamic equations from (1)–(3), ζ, P, and $\mathbf{q}$ must be specified as functionals of the fields n, T, and $\mathbf{u}$. However, some interesting results can be obtained for the purposes here even at this exact level. We emphasize that the analysis of this section and its conclusion do not depend on any specific form for the rheological equation of state, only its scaling with respect to the available hydrodynamic fields (dimensional analysis).

An idealized macroscopic state of USF is characterized by the forms [21]

$$n(\mathbf{r},t)=n,\quad T(\mathbf{r},t)=T(t),\quad u_x=ay,\quad u_y=u_z=0. \tag{4}$$

The presumed geometry is that described above. More precisely, this linear velocity profile assumes no boundary layer near the walls and is possible for special periodic boundary conditions in the local Lagrangian frame [22]. Since the density is a constant, it plays no significant role in the following and the dependence of properties on it will be suppressed. From symmetry, the cooling rate, heat flux, and pressure tensor must have the forms in the hydrodynamic state

$$\zeta=\zeta(T(t),a,\alpha),\quad \mathbf{q}=0,\quad \boldsymbol{\nabla}_j P_{ij}=0. \tag{5}$$

The balance equations (1) and (3) are satisfied exactly with these choices, while Eq. (2) becomes

$$\partial_t T(t)=-\frac{2}{dn}aP_{xy}(T(t),a,\alpha)-\zeta(T(t),a,\alpha)T(t). \tag{6}$$

The functional forms for the scalars $\zeta(T,a,\alpha)$ and $P_{xy}(T,a,\alpha)$ must be determined from a more microscopic basis. An example from kinetic theory is provided in the next section. Then, Eq. (6) provides a closed hydrodynamic equation to determine the temperature $T(t)$ for given initial condition $T(0)$ and specification of the constants a and α. The first term on the right side is positive and represents viscous heating. To make this more explicit it is usual to introduce the nonlinear shear viscosity $\eta(T,a,\alpha)$ by

$$P_{xy}(T,a,\alpha)\equiv-\eta(T,a,\alpha)a. \tag{7}$$

A Newtonian fluid is that for which the viscosity and cooling rate becomes independent of the shear rate,

$$\eta(T,a,\alpha)\to\eta(T,a=0,\alpha)\equiv\eta_0(T,\alpha),$$

$$\zeta(T,a,\alpha)\to\zeta(T,a=0,\alpha)\equiv\zeta_0(T,\alpha). \tag{8}$$

The corresponding hydrodynamic equation for a Newtonian fluid becomes

$$\partial_t T(t) = -\zeta_0(T(t),\alpha)T(t) + a^2\left[\frac{2}{dn}\eta_0(T(t),\alpha) - \zeta_2(T(t),\alpha)T(t)\right]. \quad (9)$$

Here, for consistency, the cooling rate also has been expanded to second order in the shear rate,

$$\zeta(T(t),a,\alpha) \to \zeta_0(T(t),\alpha) + a^2\zeta_2(T(t),\alpha). \quad (10)$$

The Newtonian fluid equation (9) appears quite useful as a means to measure its viscosity. First, the cooling rate $\zeta_0(T(t),\alpha)$ is determined by measuring the time dependence of $T(t)$ at different values of α at zero shear rate. Next, the same measurement is performed as a function of the shear rate to determine the combination $(2/dn)\eta_0(T(t),\alpha) - \zeta_2(T(t),\alpha)T(t)$. In the case $\zeta_2=0$ (see the next section for an example) this determines the Newtonian viscosity. Two questions arise at this point. First, can the measurement of the Newtonian viscosity be simplified by considering only the steady state? Second, under what conditions does the Newtonian limit for the steady state apply? To answer these questions we have to take into account that the domain of validity of the Newtonian description is restricted to small shear rates. To be more precise, a dimensionless shear rate must be introduced. The only other relevant frequency for the fluid is its mean collision frequency $\nu(T(t)) \propto \sqrt{T(t)}$. Consequently, the relevant dimensionless shear rate, cooling rate, and shear viscosity are defined by

$$a^*(T(t)) = \frac{a}{\nu(T(t))}, \quad \zeta^*(a^*,\alpha) = \frac{\zeta(T(t),a,\alpha)}{\nu(T(t))},$$

$$\eta^*(a^*,\alpha) = \frac{\nu(T(t))}{nT(t)}\eta(T(t),a,\alpha), \quad (11)$$

where $\zeta^*(a^*,\alpha)$ and $\eta^*(a^*,\alpha)$ can depend on time and temperature only through $a^*(T(t))$, in order to be dimensionless. Note that the reduced shear rate a^* is actually a measure of the granular temperature since $T \propto a^{*-2}$. In the steady state, Eq. (6) becomes

$$a^{*2} = \frac{d\zeta^*(a^*,\alpha)}{2\eta^*(a^*,\alpha)}. \quad (12)$$

The solution to this equation gives $a_s^*(\alpha)$, that depends only on α and thus cannot be made small by controlling the shear rate a. In general, $a_s^*(\alpha) \ll 1$ only in the quasielastic limit $1-\alpha \ll 1$,

$$a_s^{*2}(\alpha) \to \frac{d\zeta_0^*(\alpha)}{2\eta_0^*(\alpha=1)} \equiv a_0^{*2}(\alpha) \sim 1-\alpha \ll 1, \quad (13)$$

where we have taken into account that $\zeta_0^*(\alpha) \propto 1-\alpha^2 \sim 2(1-\alpha)$ in the quasielastic limit. In this case the dimensionless steady state shear viscosity becomes $\eta_s^*(\alpha) = \eta^*(a_s^*(\alpha),\alpha) \to \eta^*(a_0^*(\alpha),\alpha)$. Since, according to Eq. (13), a_0^* is small, the steady state shear viscosity is expected to differ from the dimensionless Newtonian viscosity $\eta_0^*(\alpha) = \eta^*(a^*=0,\alpha)$ by a (super-Burnett) term of order a_0^{*2}:

$$\eta_s^*(\alpha) - \eta_0^*(\alpha) \sim a_0^{*2}(\alpha) \sim 1-\alpha. \quad (14)$$

On the other hand, by expanding the Newtonian shear viscosity $\eta_0^*(\alpha)$ around its value in the elastic case, we have

$$\eta_0^*(\alpha) - \eta_0^*(\alpha=1) \sim 1-\alpha, \quad (15)$$

for small inelasticities. Therefore, Eqs. (14) and (15) show that in the quasielastic limit the steady state shear viscosity $\eta_s^*(\alpha)$ differs from the Newtonian viscosity $\eta_0^*(\alpha)$ as much as the latter differs from that of the elastic gas. This shows that a measurement of the steady state temperature to determine $a_s^*(\alpha)$ does not allow determination of the Newtonian viscosity, even for $1-\alpha \ll 1$. The α dependence of $\eta_0^*(\alpha) = \eta^*(a^*=0,\alpha)$ cannot be isolated from the α dependence of $\eta^*(a_s^*(\alpha),\alpha)$. Both viscosities coincide only in the trivial case $\alpha=1$.

In summary, for any chosen $a,\alpha,T(0)$ the steady state viscosity is $\eta^*(a_s^*(\alpha),\alpha)$ and the system samples a non-Newtonian value from the general rheological equation of state $\eta^*(a^*,\alpha)$ that is always different from the Newtonian value.

III. DESCRIPTION FROM THE BOLTZMANN KINETIC THEORY

To explore this phenomenon in more detail it is necessary to calculate the rheological equation of state $\eta^*(a^*,\alpha)$. This requires a more microscopic analysis such as kinetic theory. At low density the granular Boltzmann equation provides the appropriate starting point.

A. Boltzmann equation and Newtonian viscosity

The Boltzmann kinetic equation determines the probability density $f(\mathbf{r},\mathbf{v},t)$ for a particle to have position $\mathbf{r}$ and velocity $\mathbf{v}$ at time t in a low density gas. It has the form

$$\left(\frac{\partial}{\partial t} + \mathbf{v}\cdot\boldsymbol{\nabla}\right) f(\mathbf{r},\mathbf{v},t) = J[\mathbf{r},\mathbf{v}|f(t)]. \quad (16)$$

The right-hand side describes the effects of inelastic pair collisions. The detailed form of the Boltzmann collision operator, J, is not required here beyond noting the properties necessary for the macroscopic balance equations

$$\int d\mathbf{v} \begin{pmatrix} 1 \\ \mathbf{v} \\ \frac{1}{2}m(\mathbf{v}-\mathbf{u})^2 \end{pmatrix} J[\mathbf{r},\mathbf{v}|f(t)] = \begin{pmatrix} 0 \\ 0 \\ -\frac{d}{2}nT\zeta \end{pmatrix}. \quad (17)$$

Here the density n, the temperature T, and the macroscopic flow velocity $\mathbf{u}$ are defined in terms of $f(\mathbf{r},\mathbf{v},t)$ by

$$\begin{pmatrix} n(\mathbf{r},t) \\ n(\mathbf{r},t)\mathbf{u}(\mathbf{r},t) \\ \frac{d}{2}n(\mathbf{r},t)T(\mathbf{r},t) \end{pmatrix} = \int d\mathbf{v} \begin{pmatrix} 1 \\ \mathbf{v} \\ \frac{1}{2}m(\mathbf{v}-\mathbf{u})^2 \end{pmatrix} f(\mathbf{r},\mathbf{v},t). \quad (18)$$

The two zeros on the right-hand side of Eq. (17) correspond to conservation of mass and momentum, while the last term

results from nonconservation of energy. The properties (17) lead to the macroscopic balance equations (1)–(3), with the following microscopic expressions for the pressure tensor, the heat flux, and the cooling rate:

$$P_{ij}(\mathbf{r},t) = m \int d\mathbf{v} V_i V_j f(\mathbf{r},\mathbf{v},t), \tag{19}$$

$$\mathbf{q}(\mathbf{r},t) = \frac{m}{2} \int d\mathbf{v} V^2 \mathbf{V} f(\mathbf{r},\mathbf{v},t), \tag{20}$$

$$\zeta(\mathbf{r},t) = (1-\alpha^2) \frac{m\pi^{(d-1)/2}\sigma^{d-1}}{4d\Gamma\left(\frac{d+3}{2}\right) n(\mathbf{r},t) T(\mathbf{r},t)} \times \int d\mathbf{v} \int d\mathbf{v}_1 |\mathbf{v}-\mathbf{v}_1|^3 f(\mathbf{r},\mathbf{v},t) f(\mathbf{r},\mathbf{v}_1,t). \tag{21}$$

In Eqs. (19) and (20), $\mathbf{V}=\mathbf{v}-\mathbf{u}(\mathbf{r},t)$ is the peculiar velocity.

It is straightforward to determine the Navier-Stokes shear viscosity coefficient $\eta_0(T,\alpha)$ by using the Chapman-Enskog method [23]. The result is [20,24,25]

$$\eta_0(T,\alpha) = \frac{nT}{\nu(T)} \eta_0^*(\alpha), \tag{22}$$

where

$$\nu(T) = \frac{8\pi^{(d-1)/2}\sigma^{d-1}}{(d+2)\Gamma(d/2)} n \left(\frac{T}{m}\right)^{1/2} \tag{23}$$

is an effective collision frequency, and

$$\eta_0^*(\alpha) = \left[\beta(\alpha) + \tfrac{1}{2}\zeta_0^*(\alpha)\right]^{-1}. \tag{24}$$

Here $\zeta_0^*(\alpha)=\zeta_0/\nu$ is the dimensionless cooling rate in the homogeneous cooling state, while $\beta(\alpha)$ is a dimensionless function of the restitution coefficient given in terms of the solution to the linearized Boltzmann equation. Explicit results for ζ_0^* and β can be obtained by considering the leading terms in a Sonine polynomial expansion. In that approximation,

$$\zeta_0^*(\alpha) = \frac{d+2}{4d}(1-\alpha^2), \tag{25}$$

$$\beta(\alpha) = \frac{1+\alpha}{2}\left[1 - \frac{d-1}{2d}(1-\alpha)\right]. \tag{26}$$

B. Uniform shear flow

It becomes prohibitively difficult to go beyond Navier-Stokes order to get the exact full dependence of $\eta^*(a^*,\alpha)$ on a^* from the Boltzmann equation. On the other hand, a good estimate is provided by considering the leading Sonine approximation to the distribution function (Grad's method) [18,26].

In the special case of USF the solution to the Boltzmann kinetic equation is spatially uniform when expressed in terms of the velocity relative to the local flow, $V_x=v_x-ay$, $V_y=v_y$, $V_z=v_z$. Consequently, the Boltzmann equation (16) becomes [21]

$$\left(\partial_t - aV_y \frac{\partial}{\partial V_x}\right) f(\mathbf{V},t) = J[\mathbf{V}|f(t)]. \tag{27}$$

Multiplying both sides of Eq. (27) by mV_iV_j and integrating over velocity, we get

$$\partial_t P_{ij} + a(\delta_{ix}P_{yj} + \delta_{jx}P_{iy}) = m\int d\mathbf{v} V_i V_j J[\mathbf{V}|f] \equiv -\Lambda_{ij}. \tag{28}$$

The exact expression of the collision integral Λ_{ij} is not known, even in the elastic case. However, a good estimate can be expected by using Grad's approximation

$$f(\mathbf{V}) \to f_0(\mathbf{V})\left[1 + \frac{m}{2T}\left(\frac{P_{ij}}{nT} - \delta_{ij}\right) V_i V_j\right], \tag{29}$$

where

$$f_0(\mathbf{V}) = n(m/2\pi T)^{d/2} \exp(-mV^2/2T) \tag{30}$$

is the local equilibrium distribution function. When Eq. (29) is inserted into the definition of Λ_{ij} and terms nonlinear in $P_{ij}/nT-\delta_{ij}$ are neglected, one gets [26]

$$\Lambda_{ij} = \nu[\beta(P_{ij}-\delta_{ij}) + \zeta_0^* P_{ij}], \tag{31}$$

where ζ_0^* and β are given by Eqs. (25) and (26), respectively. It is worth noting that Eq. (31) coincides with the one obtained from a simple kinetic model [15,27].

The three relevant independent equations from (28) and (31) are

$$\partial_t p + \zeta_0 p + \frac{2a}{d} P_{xy} = 0, \tag{32}$$

$$\partial_t P_{xy} + (\beta\nu + \zeta_0) P_{xy} + a P_{yy} = 0, \tag{33}$$

$$\partial_t P_{yy} + (\beta\nu + \zeta_0) P_{yy} - \beta\nu p = 0, \tag{34}$$

where $p=nT=P_{ii}/d$ is the low density pressure. If we define the dimensionless quantities

$$P_{ij}^*(t) = \frac{P_{ij}(t)}{nT(t)}, \quad a^*(t) = \frac{a}{\nu(T(t))},$$

$$\tau(t) = \int_0^t dt' \nu(T(t')), \tag{35}$$

then Eqs. (32)–(34) become

$$2\partial_\tau \ln a^* = \zeta_0^* + \frac{2}{d} P_{xy}^* a^*, \tag{36}$$

$$\partial_\tau P_{xy}^* = -a^* P_{yy}^* - P_{xy}^*\left(\beta - \frac{2}{d} P_{xy}^* a^*\right), \tag{37}$$

$$\partial_\tau P_{yy}^* = -P_{yy}^*\left(\beta - \frac{2}{d}P_{xy}^* a^*\right) + \beta. \tag{38}$$

The variable τ is the dimensionless time measured as the average collision number. The solution to these nonlinear equations gives a^*, P_{xy}^*, and P_{yy}^* as functions of τ for a given value of α. The rheological equation of state is then obtained from

$$\eta^*(a^*(\tau)) = -\frac{P_{xy}^*(\tau)}{a^*(\tau)}. \tag{39}$$

1. Steady state solution

Consider first the steady state solution. Equation (36) gives

$$P_{xy,s}^* = -\frac{d\zeta_0^*}{2a_s^*}, \tag{40}$$

while Eqs. (37) and (38) give

$$P_{yy,s}^* = \beta(\beta + \zeta_0^*)^{-1}, \quad P_{xy,s}^* = -a_s^*\beta(\beta + \zeta_0^*)^{-2}. \tag{41}$$

The value of a^* in the steady state is obtained from Eqs. (40) and (41),

$$a_s^*(\alpha) = \sqrt{\frac{d\zeta_0^*(\alpha)}{2\beta(\alpha)}}[\beta(\alpha) + \zeta_0^*(\alpha)]. \tag{42}$$

As anticipated above, it is independent of the initial temperature and shear rate a. Appendix A shows that the steady state solution (41) and (42) is indeed a (linearly) stable solution.

The second equality in (41) allows one to identify the steady state shear viscosity as

$$\eta_s^*(\alpha) = -\frac{P_{xy}^*}{a^*} = \beta(\alpha)[\beta(\alpha) + \zeta_0^*(\alpha)]^{-2}. \tag{43}$$

This gives the explicit form for the steady state shear viscosity, showing it is also independent of the shear rate a and the initial temperature. Furthermore, its dependence on α is qualitatively different from that of Eq. (24) for a Newtonian fluid. This is illustrated in Fig. 1, which also shows that the analytical results compare favorably well with simulation data obtained from the direct simulation Monte Carlo (DSMC) method [28,29]. Clearly, there is no relationship of the steady state shear viscosity to the Newtonian viscosity at any value of α. While the Newtonian viscosity is $\eta_0^*(\alpha) > 1$, the steady state viscosity is $\eta_s^*(\alpha) < 1$. In the quasielastic limit, Eqs. (24), (42), and (43) yield

$$\eta_0^*(\alpha) \to 1 + \frac{3d-4}{4d}(1-\alpha), \tag{44}$$

$$a_s^{*2}(\alpha) \to a_0^{*2}(\alpha) = \frac{d+2}{4}(1-\alpha), \tag{45}$$

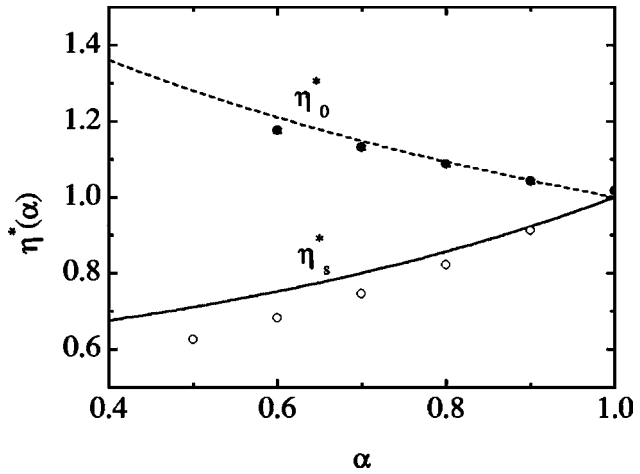

FIG. 1. Plot of the dimensionless Newtonian shear viscosity $\eta_0^*(\alpha)$ (dashed line) and the dimensionless steady state shear viscosity $\eta_s^*(\alpha)$ (solid line) for $d=3$, as given by Eqs. (24) and (43), respectively. Filled circles [28] and open circles [29] represent simulation data obtained from the numerical solution of the Boltzmann equation by the DSMC method.

$$\eta_s^*(\alpha) \to 1 - \frac{5}{2d}(1-\alpha). \tag{46}$$

Equations (44)–(46) confirm the qualitative arguments behind Eqs. (13)–(15). Eliminating α between Eqs. (45) and (46), one has

$$\eta_s^*(\alpha) \to 1 - \frac{10}{d(d+2)}a_s^{*2}(\alpha) \tag{47}$$

in the quasielastic limit.

2. Unsteady hydrodynamic solution

The more general solution to Eqs. (36)–(38) corresponding to hydrodynamics is that for which all time dependence occurs through the hydrodynamic fields (the Chapman-Enskog "normal" solution). The time dependence is due only to the temperature for USF which occurs in the dimensionless forms above through their dependence on $a^*(t) = a/\nu(T(t))$,

$$\partial_\tau P_{ij}^* = \frac{\partial P_{ij}^*}{\partial a^*}\partial_\tau a^*. \tag{48}$$

Then, using Eq. (36), Eqs. (37) and (38) become

$$\frac{\partial P_{xy}^*}{\partial a^*} = \frac{-2P_{yy}^* - \frac{2}{a^*}P_{xy}^*\left(\beta - \frac{2}{d}P_{xy}^* a^*\right)}{\zeta_0^* + \frac{2}{d}P_{xy}^* a^*}, \tag{49}$$

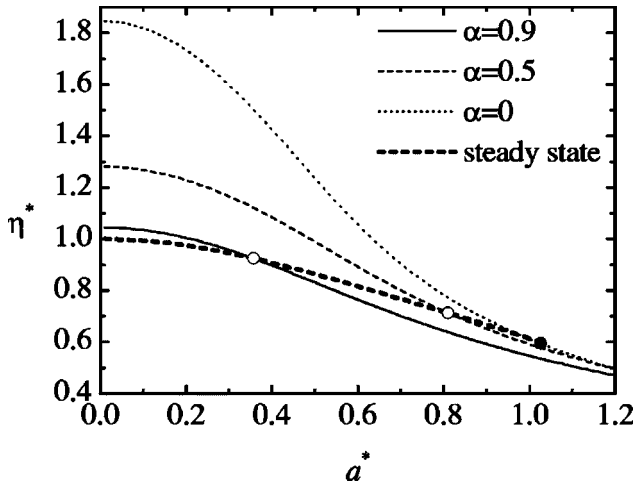

FIG. 2. Plot of $\eta^*(a^*,\alpha)$ as a function of a^* for $d=3$ and $\alpha=0.9$ (solid line), $\alpha=0.5$ (dashed line), and $\alpha=0$ (dotted line). The thick dashed line is the locus of points (a_s^*,η_s^*), which are parametrically found from Eqs. (42) and (43). It intercepts the curves representing $\eta^*(a^*,\alpha)$ at the steady state values (indicated by circles). Note that the curve (a_s^*,η_s^*) ends at the point corresponding to $\alpha=0$ (represented by a filled circle).

$$\frac{\partial P_{yy}^*}{\partial a^*}=\frac{2\beta-2P_{yy}^*\left(\beta-\frac{2}{d}P_{xy}^*a^*\right)}{a^*\left(\zeta_0^*+\frac{2}{d}P_{xy}^*a^*\right)}. \tag{50}$$

This is a set of two coupled nonlinear differential equations that must be solved with the appropriate boundary conditions to get the *hydrodynamic* solution. There is a singular point corresponding to the steady state solution (41) and (42), in which case the numerators and denominators of Eqs. (49) and (50) vanish.

The unsteady hydrodynamic solutions $\eta^*(a^*,\alpha)=-P_{xy}^*/a^*$ are illustrated in Fig. 2 for three different values of α. Also shown are the special values of the steady state shear rate $a_s^*(\alpha)$ and shear viscosity $\eta_s^*(\alpha)$ for each curve. For each value of α the point (a_s^*,η_s^*) splits the curve $\eta^*(a^*)$ into two physically different branches, one for $a^*<a_s^*$ and another one for $a^*>a_s^*$. Suppose that for a given shear rate a and initial temperature $T(0)$ the value of a^* is less than that for the steady state, $a^*(0)=a/\nu(T(0))<a_s^*$. The cooling dominates viscous heating in this case and the temperature decreases, leading to a larger value of $a^*(\tau)$. In this way, the system evolves according to the hydrodynamic equations along the curve until the steady state value a_s^* is attained, i.e., $a^*(\tau)\to a_s^*$ as $\tau\to\infty$. A parametric plot of $\eta^*(\tau)$ versus $a^*(\tau)$ gives the branch of the curve $\eta^*(a^*)$ corresponding to $a^*<a_s^*$. Analogously, a heating process occurs in the opposite case of an initial value for a^* greater than that for the steady state until $\lim_{\tau\to\infty}a^*(\tau)=a_s^*$ again. This provides the branch corresponding to $a^*>a_s^*$. As an example, Fig. 3 shows the time evolution of $a^*(\tau)\propto 1/\sqrt{T(\tau)}$, $-P_{xy}^*(\tau)$, and $P_{yy}^*(\tau)$ for $\alpha=0.5$ and two different initial conditions: (i) $a^*(0)=0.1$, $P_{xy}^*(0)=-0.1$, $P_{yy}^*(0)=1$, and (ii) $a^*(0)=2$, $P_{xy}^*(0)=-0.5$, $P_{yy}^*(0)=0.4$. In both cases, after about 20–30 collisions per particle, the system reaches a common steady state with $a_s^*=0.812$, $-P_{xy,s}^*=0.577$, and $P_{yy,s}^*=0.667$. We have checked that the same asymptotic state is achieved when starting from different initial conditions.

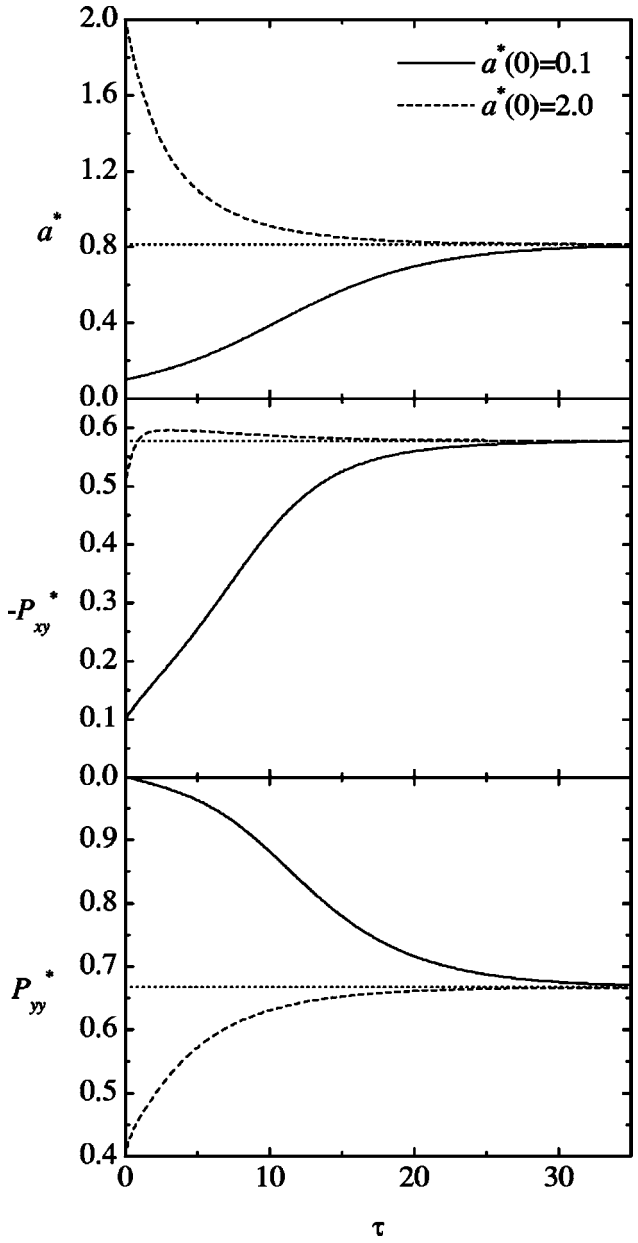

FIG. 3. Time evolution of the reduced shear rate $a^*(\tau)$, the reduced shear stress $-P_{xy}^*(\tau)$, and the reduced normal stress $P_{yy}^*(\tau)$ for $d=3$, $\alpha=0.5$, and two different initial conditions: (i) $a^*(0)=0.1$, $P_{xy}^*(0)=-0.1$, $P_{yy}^*(0)=1$ (solid lines), and (ii) $a^*(0)=2$, $P_{xy}^*(0)=-0.5$, $P_{yy}^*(0)=0.4$ (dashed lines). The horizontal dotted lines represent the steady state values $a_s^*=0.812$, $-P_{xy,s}^*=0.577$, and $P_{yy,s}^*=0.667$.

In order to get the branch of the hydrodynamic solution corresponding to $a^*<a_s^*$ one must apply the physical boundary condition

$$\lim_{a^*\to 0} \eta^*(a^*,\alpha) = \eta_0^*(\alpha), \quad \lim_{a^*\to 0} P_{yy}^*(a^*,\alpha) = 1. \tag{51}$$

In practice, the branch $a^* < a_s^*$ for each curve of Fig. 2 has been obtained by solving numerically the coupled set (49) and (50) with the initial condition

$$P_{xy}^* = -\eta_0 a^*(0), \quad P_{yy}^* = 1 \tag{52}$$

with $a^*(0) = 10^{-5}$.

As said before, the branch corresponding to $a^* > a_s^*$ is inaccessible starting from an initial value $a^*(0) < a_s^*$. Therefore, in order to obtain $\eta^*(a^*)$ for $a^* > a_s^*$, one must take the boundary condition at the point at infinity. For that case, simple physical intuition is not enough to determine the appropriate boundary conditions, so one must resort to a detailed asymptotic analysis of Eqs. (49) and (50). Such an analysis is carried out in Appendix B, where we find that $-P_{xy}^* \sim a^{-1/3}$, $P_{yy}^* \sim a^{-2/3}$ for asymptotically large a^*. More specifically, if the shear rate a^* is much larger than 1, then

$$P_{xy}^* = -\left(\frac{9d^2\beta}{56}\right)^{1/3} a^{*-1/3}, \tag{53a}$$

$$P_{yy}^* = \left(\frac{21d\beta^2}{64}\right)^{1/3} a^{*-2/3}. \tag{53b}$$

The branch $a^* > a_s^*$ in Fig. 2 has been obtained from the numerical solution of the coupled set (49) and (50) with the initial conditions (53) with $a^*(0) = 10$.

IV. DISCUSSION

The primary observation here has been that granular fluids admit hydrodynamic steady states that are inherently beyond the scope of the Navier-Stokes or Newtonian hydrodynamic equations. The reason for this is the existence of an internal mechanism, collisional cooling, that sets the scale of the spatial gradients in the steady state. For normal fluids, this scale is set by external sources (boundary conditions, driving forces) that can be controlled to admit the conditions required for Navier-Stokes hydrodynamics. In contrast, collisional cooling is fixed by the mechanical properties of the particles making up the fluid. An example is a sheared fluid where the work done at the boundaries is balanced by a combination of collisional cooling and internal heat flux. To illustrate and emphasize these effects in more detail and quantitatively, we have considered the idealized state of uniform shear flow (USF), for which no heat flux occurs. The Lees-Edwards boundary conditions generating USF cannot be applied in experimental conditions, although they can be easily implemented in computer simulations. However, even for the laboratory conditions of Couette flow the cooling rate will still be a function of the hydrodynamic gradients leading to similar non-Newtonian behavior.

In spite of the extensive prior work on USF for granular fluids, the observation about its inherent non-Newtonian character is apparently new although implicit in results obtained from various models (e.g., the observation that $a^{*2} \sim 1-\alpha$). This is significant because molecular dynamics simulation of steady USF has been used for real fluids to measure the Newtonian shear viscosity. The analysis here shows that this is not possible for granular fluids. More generally, it provides a caution regarding the simulation of other steady states to study Navier-Stokes hydrodynamics when the gradients are strongly correlated to the collisional cooling. On a more positive note, these results show that USF is an ideal testing ground for the study of rheology since any choice of the shear rate and α will provide non-Newtonian effects. It is one of the fascinating features of granular fluids that phenomena associated with complex fluids are more easily accessible than for simple atomic fluids [30].

The macroscopic state of steady uniform shear flow is simple in the sense that it is spatially uniform in the local Lagrangian frame, and the only hydrodynamic gradient is that of the velocity field characterized by the scalar shear rate a. Non-Newtonian effects occur through the dependence of the shear viscosity on the shear rate. The condition for a steady state is an exact balance between viscous heating and collisional cooling. It is shown in Sec. II that this implies a value of the appropriate dimensionless shear rate that is fixed by the restitution coefficient. Hence, it is not possible to make this hydrodynamic gradient small, as required for the Newtonian limit, by any initial control of a or the initial temperature. Further quantitative illustration of this is given in Sec. III where the shear rate dependence of the shear viscosity is determined from an approximate Grad's solution of the Boltzmann equation. The temporal approach to the steady state via cooling or heating proceeds along a rheological equation of state shown in Fig. 2, but the final steady state is independent of the initial conditions and lies in the non-Newtonian domain for any value of the restitution coefficient $\alpha \neq 1$. One consequence is that experimental or simulation measurements in steady USF provide no information about Navier–Stokes transport.

This phenomenon of peculiar steady states for granular fluids extends to other states as well. The steady state macroscopic balance equations are

$$\boldsymbol{\nabla}\cdot(n\mathbf{u}) = 0, \tag{54}$$

$$-\mathbf{u}\cdot\boldsymbol{\nabla}\ln T - \frac{2}{dnT}(P_{ij}\nabla_j u_i + \boldsymbol{\nabla}\cdot\mathbf{q}) = \zeta, \tag{55}$$

$$\mathbf{u}\cdot\boldsymbol{\nabla}u_i + (mn)^{-1}\nabla_j P_{ij} = 0. \tag{56}$$

In the absence of collisional cooling the spatial gradients can be sustained only by boundary conditions or external forces. However, for finite ζ spatial gradients can exist that are not controlled by such external sources and their size may preclude the validity of simple Navier-Stokes hydrodynamics. Each physical state should be checked for this possibility.

As another simple example, consider the steady state of a granular gas enclosed between two parallel plates at rest and maintained at the same temperature. For elastic particles such a steady state is trivially that of equilibrium at the wall temperature. Nevertheless, for a granular gas the collisional dissipation induces a heat flux, cf. Eq. (55), and hence a thermal gradient, along with a density gradient, exists

[31–33]. In the quasielastic limit, the kinetic model of the Boltzmann equation proposed in Ref. [27] admits a solution characterized by a constant pressure $p=nT$ and a heat flux given by [34]

$$\mathbf{q} = -\frac{d+2}{2}\frac{p}{m\nu}\lambda_s^*(\alpha)\,\boldsymbol{\nabla} T, \tag{57}$$

where

$$\lambda_s^*(\alpha) \to 1 + \frac{29d^2+116d-28}{4d(d+2)}(1-\alpha). \tag{58}$$

On the other hand, the expression for the heat flux in the Navier-Stokes order given by the Chapman-Enskog expansion is [20,24,25]

$$\mathbf{q} = -\lambda_0(\alpha)\,\boldsymbol{\nabla} T - \mu_0(\alpha)\,\boldsymbol{\nabla} n = -\frac{d+2}{2}\frac{p}{m\nu}\overline{\lambda}_0^*(\alpha)\,\boldsymbol{\nabla} T, \tag{59}$$

where λ_0 is the thermal conductivity, μ_0 is a transport coefficient with no analog in the elastic case, and in the last step we have taken into account that $\boldsymbol{\nabla} p=\mathbf{0}$, so that $\boldsymbol{\nabla} n=-(n/T)\boldsymbol{\nabla} T$. The expression for the dimensionless effective thermal conductivity $\overline{\lambda}_0^*(\alpha)$ in the quasielastic limit is

$$\overline{\lambda}_0^*(\alpha) \to 1 + \frac{3d-4}{4d}(1-\alpha). \tag{60}$$

Equations (58) and (60) clearly show that $\lambda_s^*(\alpha) \neq \overline{\lambda}_0^*(\alpha)$. In the three-dimensional case, for instance, the coefficient of $1-\alpha$ in $\lambda_s^*(\alpha)$ is about 20 times larger than that of $\overline{\lambda}_0^*(\alpha)$. Therefore, the Navier-Stokes transport coefficients do not describe correctly the heat flux in the steady state, except again in the trivial case of elastic collisions.

ACKNOWLEDGMENTS

A.S. and V.G. acknowledge partial support from the Ministerio de Ciencia y Tecnología (Spain) through Grant No. FIS2004-01399. The research of J.W.D. was supported by Department of Energy Grant Nos. DE-FG03-98DP00218 and DE-FG02ER54677.

APPENDIX A: LINEAR STABILITY ANALYSIS OF THE STEADY STATE SOLUTION

In this Appendix we carry out a linear stability analysis of the steady state solution (41) and (42) of the set of evolution equations (36)–(38). First, we write

$$a^*(\tau) = a_s^* + \delta a^*(\tau), \quad P_{xy}^*(\tau) = P_{xy,s}^* + \delta P_{xy}^*(\tau),$$

$$P_{yy}^*(\tau) = P_{yy,s}^* + \delta P_{yy}^*(\tau). \tag{A1}$$

Substituting (A1) into Eqs. (36)–(38) and neglecting nonlinear terms, one gets

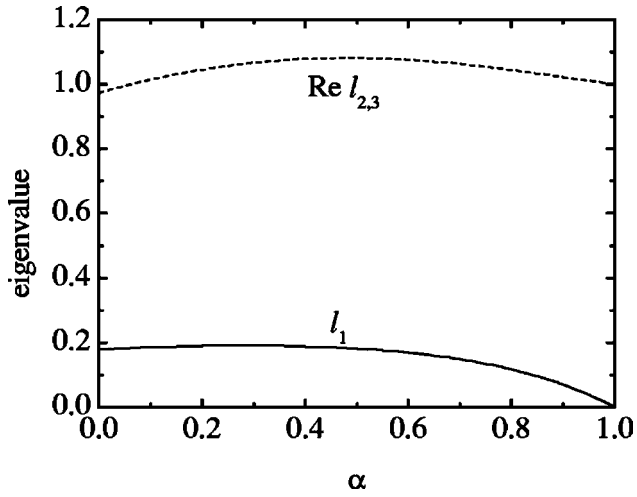

FIG. 4. Plot of the eigenvalue ℓ_1 and of the real part of $\ell_{2,3}$ as a function of the coefficient of restitution in the three-dimensional case.

$$\partial_\tau \begin{pmatrix} \delta a^* \\ \delta P_{xy}^* \\ a_s^* \delta P_{yy}^* \end{pmatrix} = -\mathsf{L}\cdot \begin{pmatrix} \delta a^* \\ \delta P_{xy}^* \\ a_s^* \delta P_{yy}^* \end{pmatrix}, \tag{A2}$$

where L is the matrix

$$\mathsf{L} = \begin{pmatrix} \zeta_0^*/2 & -\zeta_0^*(\beta+\zeta_0^*)^2/2\beta & 0 \\ \beta^2/(\beta+\zeta_0^*)^2 & \beta+2\zeta_0^* & 1 \\ \beta\zeta_0^*/(\beta+\zeta_0^*) & -\zeta_0^*(\beta+\zeta_0^*) & \beta+\zeta_0^* \end{pmatrix}. \tag{A3}$$

In Eq. (A3) use has been made of the explicit expressions (41) and (42) for the steady state solution. The time evolution of the deviations from the steady solution is governed by the eigenvalues of L. If the real parts of those eigenvalues are positive the steady solution is linearly stable, while it is unstable otherwise. The solution of the characteristic equation $\det(L_{ij}-\ell\delta_{ij})=0$ yields a real eigenvalue ℓ_1 and a pair of complex conjugate eigenvalues ℓ_2, ℓ_3. We have verified that ℓ_1 and the real parts of $\ell_{2,3}$ are positive definite for all values of the coefficient of restitution $\alpha<1$, ℓ_1 being smaller than Re $\ell_{2,3}$. Consequently, the steady state solution is stable, and the characteristic relaxation time (measured by the number of collisions) is ℓ_1^{-1}. As an illustration, Fig. 4 shows the α-dependence of ℓ_1 and Re $\ell_{2,3}$ for $d=3$. It is interesting to note that $\ell_1\to 0$ in the elastic limit $\alpha\to 1$. This is a consequence of the fact that there is no steady solution at $\alpha=1$, namely $a^*(\tau)$ decays algebraically as $a^*(\tau)\approx(2\tau/d)^{-1/2}$.

The above stability analysis is restricted to small deviations from the steady state solution. The proof that the steady state solution is an attractor as $\tau\to\infty$ for any uniform (in the Lagrangian frame) initial condition seems to be quite difficult, so that one has to resort to numerical evidence. As was illustrated in Fig. 3, the numerical results confirm that the steady state is indeed an attractor.

APPENDIX B: HYDRODYNAMIC SOLUTION FOR LARGE SHEAR RATES

In this Appendix we will get the asymptotic behavior of the solution to Eqs. (49) and (50) for large values of the reduced shear rate a^*. On physical grounds, the asymptotic solution must have the general form,

$$P_{xy}^* \approx -A_1 a^{*-b_1}, \quad P_{yy}^* \approx A_2 a^{*-b_2}, \tag{B1}$$

where $A_1>0$, $A_2>0$, and $b_2 \geqslant 0$. Inserting (B1) into Eqs. (49) and (50), one has

$$\left[2\beta - b_1\zeta_0^* + \frac{2(b_1+2)}{d}A_1 a^{*1-b_1}\right]A_1 a^{*-1-b_1} = 2A_2 a^{*-b_2}, \tag{B2}$$

$$\left[2\beta - b_2\zeta_0^* + \frac{2(b_2+2)}{d}A_1 a^{*1-b_1}\right]A_2 a^{*-b_2} = 2\beta. \tag{B3}$$

In order to carry out a balance analysis of the leading terms in (B2) and (B3), it is convenient to consider separately the cases $b_1>1$, $b_1=1$, and $b_1<1$. If $b_1>1$, then $a^{*1-b_1}\to 0$ and Eqs. (B2) and (B3) become

$$(2\beta - b_1\zeta_0^*)A_1 a^{*-1-b_1} = 2A_2 a^{*-b_2}, \tag{B4}$$

$$(2\beta - b_2\zeta_0^*)A_2 a^{*-b_2} = 2\beta. \tag{B5}$$

Equation (B4) implies that $b_2=b_1+1>2$, while Eq. (B5) yields $b_2=0$ and $A_2=1$. Therefore, Eqs. (B4) and (B5) are mutually inconsistent. The next possibility is $b_1=1$. This gives

$$\left(2\beta - \zeta_0^* + \frac{6}{d}A_1\right)A_1 a^{*-2} = 2A_2 a^{*-b_2}, \tag{B6}$$

$$\left[2\beta - b_2\zeta_0^* + \frac{2(b_2+2)}{d}A_1\right]A_2 a^{*-b_2} = 2\beta. \tag{B7}$$

According to Eqs. (B6) and (B7), $b_2=2$ and $b_2=0$, respectively, which is again inconsistent.

Finally, we consider the case $b_1<1$, so that Eqs. (B2) and (B3) reduce to

$$\frac{b_1+2}{d}A_1^2 a^{*-2b_1} = A_2 a^{*-b_2}, \tag{B8}$$

$$\frac{b_2+2}{d}A_1 A_2 a^{*1-b_1-b_2} = \beta. \tag{B9}$$

These two equations are consistent provided that

$$b_1 = \tfrac{1}{3}, \quad b_2 = \tfrac{2}{3}, \tag{B10}$$

$$A_1 = \left(\frac{9d^2\beta}{56}\right)^{1/3}, \quad A_2 = \left(\frac{21d\beta^2}{64}\right)^{1/3}. \tag{B11}$$

Therefore, for large reduced shear rates,

$$P_{xy}^* \approx -\left(\frac{9d^2\beta}{56}\right)^{1/3} a^{*-1/3}, \tag{B12}$$

$$P_{yy}^* \approx \left(\frac{21d\beta^2}{64}\right)^{1/3} a^{*-2/3}. \tag{B13}$$

It is interesting to remark that $|P_{xy}^*|\to 0$ both for small and large shear rates. Thus, $|P_{xy}^*|$ exhibits a nonmonotonic dependence on a^* characterized by a maximum value $|P_{xy}^*|_{\max}$ at a certain value $a_{\max}^*$ of the reduced shear rate. For instance, in the three-dimensional case we have found $(a_{\max}^*, |P_{xy}^*|_{\max}) = (0.64, 0.634)$, $(1.22, 0.595)$, and $(1.81, 0.579)$ for $\alpha=0$, 0.5, and 0.9, respectively. A similar nonmonotonic behavior of $|P_{xy}^*|$ occurs in the elastic case as well [21].

[1] C. S. Campbell, Annu. Rev. Fluid Mech. **22**, 57 1990.
[2] I. Goldhirsch, Annu. Rev. Fluid Mech. **35**, 267 2003.
[3] M. Tij, E. Tahiri, J. M. Montanero, V. Garzó, A. Santos, and J. W. Dufty, J. Stat. Phys. **103**, 1035 (2001).
[4] O. R. Walton and R. L. Braun, J. Rheol. **30**, 949 (1986); Acta Mech. **63**, 73 (1986).
[5] C. S. Campbell, J. Fluid Mech. **203**, 449 (1986).
[6] M. A. Hopkins and H. H. Shen, J. Fluid Mech. **244**, 477 (1992).
[7] I. Goldhirsch and M. L. Tan, Phys. Fluids **8**, 1753 (1996).
[8] A. Frezzotti, Physica A **278**, 161 (2000).
[9] M. Alam and C. M. Hrenya, Phys. Rev. E **63**, 061308 (2001).
[10] M. Alam and S. Luding, J. Fluid Mech. **476**, 69 (2003).
[11] C. K. K. Lun, S. B. Savage, D. J. Jeffrey, and N. Chepurniy, J. Fluid Mech. **140**, 223 (1984).
[12] J. T. Jenkins and M. W. Richman, J. Fluid Mech. **192**, 313 (1988).
[13] C.-S. Chou and M. W. Richman, Physica A **259**, 430 (1998); C.-S. Chou, *ibid.* **287**, 127 (2000); **290**, 341 (2001).
[14] N. Sela N., I. Goldhirsch, and S. H. Noskowicz, Phys. Fluids **8**, 2337 (1996).
[15] J. J. Brey, M. J. Ruiz-Montero, and F. Moreno, Phys. Rev. E **55**, 2846 (1997).
[16] J. M. Montanero, V. Garzó, A. Santos, and J. J. Brey, J. Fluid Mech. **389**, 391 (1999).
[17] R. Clelland and C. M. Hrenya, Phys. Rev. E **65**, 031301 (2002).
[18] J. M. Montanero and V. Garzó, Physica A **310**, 17 (2002).
[19] J. M. Montanero and V. Garzó, Mol. Simul. **29**, 357 (2003).
[20] J. J. Brey, J. W. Dufty, C. S. Kim, and A. Santos, Phys. Rev. E **58**, 4638 (1998).
[21] V. Garzó and A. Santos, *Kinetic Theory of Gases in Shear Flows. Nonlinear Transport* (Kluwer Academic, Dordrecht, 2003).
[22] A. W. Lees and S. F. Edwards, J. Phys. C **5**, 1921 (1972).
[23] S. Chapman and T. G. Cowling, *The Mathematical Theory of Nonuniform Gases* (Cambridge University Press, Cambridge, 1970).

[24] V. Garzó and J. W. Dufty, Phys. Rev. E **59**, 5895 (1999).
[25] J. J. Brey and D. Cubero, in *Granular Gases*, Lecture Notes in Physics, edited by T. Pöschel and S. Luding (Springer-Verlag, Berlin, 2001), pp. 59–78.
[26] V. Garzó, Phys. Rev. E **66**, 021308 (2002).
[27] J. J. Brey, J. W. Dufty, and A. Santos, J. Stat. Phys. **97**, 281 (1999).
[28] J. M. Montanero, A. Santos, and V. Garzó (unpublished).
[29] A. Astillero and A. Santos (unpublished).
[30] I. Goldhirsch, in *Granular Gases*, Lecture Notes in Physics, edited by T. Pöschel and S. Luding (Springer-Verlag, Berlin, 2001), pp. 79–99.
[31] J. J. Brey and D. Cubero, Phys. Rev. E **57**, 2019 (1998).
[32] R. Soto, M. Mareschal, and D. Risso, Phys. Rev. Lett. **83**, 5003 (1999).
[33] R. Ramírez, D. Risso, R. Soto, and P. Cordero, Phys. Rev. E **62**, 2521 (2000).
[34] V. Garzó, A. Santos, and J. W. Dufty (unpublished).